Non-destructive estimates of soil carbonic anhydrase activity and associated soil water oxygen isotope composition

Sam P. Jones[1], Jérôme Ogée[1], Joana Sauze[1], Steven Wohl[1], Noelia Saavedra[1], Noelia Fernández-Prado[1], Juliette Maire[1], Thomas Launois[1], Alexandre Bosc[1], and Lisa Wingate

5   [1]

[1] INRA, UMR ISPA, F-33140, Villenave d'Ornon, France

Correspondence to: Sam Jones (samuel.jones@inra.fr)

Abstract

10   The contribution of photosynthesis and soil respiration to net land-atmosphere carbon dioxide (CO_2) exchange can be estimated based on the differential influence of leaves and soils on budgets of the oxygen isotope composition ($\delta^{18}O$) of atmospheric CO_2. To do so, the activity of carbonic anhydrases (CA), a group of enzymes that catalyse the hydration of CO_2 in soils and plants, needs to be understood. Measurements of soil CA activity typically involve the inversion of models describing the $\delta^{18}O$ of CO_2 fluxes to solve for the apparent, potentially catalysed, rate of CO_2 hydration. This requires
15   information about the $\delta^{18}O$ of CO_2 in isotopic equilibrium with soil water, typically obtained from destructive, depth-resolved sampling and extraction of soil water. In doing so, an assumption is made about the soil water pool that CO_2 interacts with, that may bias estimates of CA activity if incorrect. Furthermore, this can represent a significant challenge in data collection given the potential for spatial and temporal variability in the $\delta^{18}O$ of soil water and limited *a priori* information with respect to the appropriate sampling resolution and depth. We investigated whether we could circumvent this
20   requirement by inferring the rate of CO_2 hydration and the $\delta^{18}O$ of soil water from the relationship between the $\delta^{18}O$ of CO_2 fluxes and the $\delta^{18}O$ of CO_2 at the soil surface measured at different ambient CO_2 conditions. This approach was tested through laboratory incubations of air-dried soils that were re-wetted with three waters of different $\delta^{18}O$. Gas exchange measurements were made on these soils to estimate the rate of hydration and the $\delta^{18}O$ of soil water, followed by soil water extraction to allow for comparison. Estimated rates of CO_2 hydration were 6.8 to 14.6 times greater than the theoretical un-
25   catalysed rate of hydration, indicating that CA were active in these soils. Importantly, these estimates were not significantly different among water treatments suggesting that this represents a robust approach to assay the activity of CA in soil. As expected, estimates of the $\delta^{18}O$ of the soil water that equilibrates with CO_2 varied in response to alteration to the $\delta^{18}O$ of soil water. However, these estimates were consistently more negative than the composition of the soil water extracted by cryogenic vacuum distillation at the end of the gas measurements with differences of up to -3.94 ‰ VSMOW-SLAP. These

offsets suggest that, at least at lower water contents, CO_2-H_2O isotope equilibration primarily occurs with water pools that are bound to particle surfaces and are depleted in ^{18}O compared to bulk soil water.

1 Introduction

Carbonic anhydrases (CA) are a group of metalloenzymes, typically utilising either zinc (Hewett-Emmett and Tashian, 1996) or cadmium (Xu et al., 2008), that catalyse the reversible hydration of dissolved carbon dioxide (CO_2). Spread amongst at least five unrelated classes, these enzymes have been identified in eukarya, bacteria and archaea (Gilmour, 2010). Such convergent evolution among diverse groups of organisms suggests that CA are fundamental to many life strategies (Smith et al., 1999). Indeed, these enzymes have been linked to a number of common and specialised biological processes, such as CO_2 concentration mechanisms required to maintain photosynthesis in plants, algae and cyanobacteria (Badger, 2003; Badger and Price, 1994), calcification to limit calcium toxicity in bacteria (Banks et al., 2010; Li et al., 2005b), maintenance of required CO_2 and bicarbonate levels for metabolic activity in both bacteria (Merlin et al., 2003) and fungi (Kaur et al., 2009) growing under CO_2 limited conditions, and metabolic flexibility in methanogenic archaea (Smith and Ferry, 2000). However, despite evidence of CA activity in soils, the variability and drivers of their expression by soil communities is poorly understood (Li et al., 2005a; Seibt et al., 2006; Wingate et al., 2009, 2008).

This knowledge gap is of particular importance as soil CA activity can considerably alter the oxygen isotope composition ($\delta^{18}O$) of atmospheric CO_2 (Stern et al., 2001; Tans, 1998; Wingate et al., 2009). The presence of CA in soils and leaves influences the $\delta^{18}O$ of atmospheric CO_2 as oxygen isotopes are exchanged between CO_2 and water during CA-catalysed hydration (Mills and Urey, 1940; Uchikawa and Zeebe, 2012). The $\delta^{18}O$ of soil water (δ_{sw}) and leaf water pools are typically distinct because of differences in pool sizes and evaporation rates, and these different signals are transferred to dissolved CO_2 molecules (Farquhar et al., 1993; Francey and Tans, 1987; Stern et al., 2001). This leads to contrasted $\delta^{18}O$ signatures of soil-atmosphere (δ_R) and leaf-atmosphere CO_2 exchange that can be used to partition the contribution of photosynthesis and soil respiration, the largest gross fluxes in the contemporary atmospheric carbon cycle (Ciais et al., 2013), to the net atmospheric CO_2 budget (Welp et al., 2011; Yakir and Wang, 1996). Whilst the extent to which the $\delta^{18}O$ of CO_2 interacting with leaves approaches equilibrium with leaf water pools has been considered (Gillon and Yakir, 2001), the degree to which the catalysis of CO_2 hydration by CA in soils influences δ_R is less well understood (Wingate et al., 2009). As such, appropriately modelling budgets of the $\delta^{18}O$ of atmospheric CO_2 relies on improving our knowledge of soil CA activity. In this respect, a better understanding of soil CA activity not only represents a frontier in soil ecology but also in understanding interactions between soil hydrological and carbon cycles, and ecosystem function within the carbon cycle at much larger scales.

A number of methods have been developed to estimate CA activity. Conventionally, assays have expressed activity by comparing the time required to achieve a set pH change in a CO_2-saturated buffer solution in the presence and absence of

CA-containing extracts (Wilbur and Anderson, 1948). Whilst this approach has been applied to soils (Li et al., 2005a), the requirement to work with enzyme extractions at low temperatures implies that activity is being estimated under extremely disturbed conditions. Less disruptive isotope labelling techniques, that estimate the rate of hydration and thus CA activity based on the loss of the label from an $\delta^{18}O$-enriched CO_2 source (Mills and Urey, 1940; Tu et al., 1978) have also been

5   applied to studies of aquatic algae (Hopkinson et al., 2013). Similarly, soil studies have focused on inverting models that describe δ_R (Miller et al., 1999; Tans, 1998) to assay CA activity under realistic conditions from natural abundance gas flux measurements (Kapiluto et al., 2007; Seibt et al., 2006; Wingate et al., 2008). Following Tans (1998) for a semi-infinite soil column with constant conditions throughout the depth profile, δ_R (‰ Vienna Pee Dee Belemnite CO_2 ($VPDB_g$)) at steady state can be described as (see also Wingate et al., 2010):

$$\delta_R = -\frac{v_{inv} C_a}{F_R}\delta_a + \frac{v_{inv} C_a}{F_R}\delta_{eq} + \delta_{eq} - a$$

(1)

where δ_{eq} (‰ $VPDB_g$) is the $\delta^{18}O$ of CO_2 in isotopic equilibrium with soil water, a (8.8 ‰) is the isotopic fractionation associated with the diffusion of $^{12}C^{16}O^{18}O$ in still air, v_{inv} (m s^{-1}) is the so-called piston or invasion velocity of CO_2, C_a (µmol m^{-3}) is the concentration of CO_2 in the air at the soil-air interface, F_R (µmol m^{-2} s^{-1}) is the net soil-atmosphere CO_2 flux and δ_a (‰ $VPDB_g$) is the $\delta^{18}O$ of CO_2 at the soil-air interface. The rate of ^{18}O exchange between CO_2 and soil water (k_{iso} (s^{-1})) can be

15   deduced from v_{inv} as:

$$k_{iso} = \frac{v_{inv}^2}{B\theta_w\kappa\phi_a D}$$

(2)

where B (m^3 m^{-3}) is the solubility coefficient for CO_2 in water, θ_w (m^3 m^{-3}) is the volumetric soil water content, κ is the tortuosity of the soil pore network, ϕ_a is the soil air-filled porosity and D (m^2 s^{-1}) is the molecular diffusivity of $^{12}C^{16}O^{18}O$ in air. The activity of CA is then estimated from k_{iso} using rate constants (Mills and Urey, 1940; Uchikawa and Zeebe, 2012).

20   Either as the equivalent CA concentration required to achieve the observed k_{iso} assuming known enzymatic parameters (Ogée et al., 2016; Uchikawa and Zeebe, 2012) or as the unit-less enhancement factor between k_{iso} and the theoretical un-catalysed rate of CO_2-H_2O isotopic exchange (Seibt et al., 2006; Wingate et al., 2009, 2008). In the first instance, deducing a CA concentration is hampered by the paucity of information regarding the variability of CA kinetic parameters at the bulk soil scale (Ogée et al., 2016) as communities of fungi, algae, bacteria and archaea are likely to express a mixture of α, β and γ-

25   CA classes (Gilmour, 2010; Smith and Ferry, 2000). The second approach has been used to describe temporal variations in CA activity (Seibt et al., 2006; Wingate et al., 2010, 2008), but its meaning is not always intuitive when applied across soil types as the un-catalysed rate of exchange is pH dependent (Uchikawa and Zeebe, 2012). This aside, solving Eq. 1 also requires δ_{eq} to be determined from depth-resolved knowledge about δ_{sw} (Wingate et al., 2009). In practice, δ_{sw} has been

assumed to be relatively constant over short periods and either extrapolated from proximal sampling (Seibt et al., 2006; Wingate et al., 2009, 2008) or set by irrigating dried soils with water of known isotopic composition (Kapiluto et al., 2007). Over longer periods, the development of δ_{sw} vertical profiles has also been estimated using soil water isotope transport models forced by meteorological data (Wingate et al., 2010). The appropriate value for δ_{eq} is then conceptually related to the

5   shallowest depth at which respired or atmospheric CO_2 has sufficient time to fully equilibrate with soil water (Miller et al., 1999; Wingate et al., 2009). For example, Wingate et al. (2009) estimate this depth as the soil depth below which $^{12}C^{16}O^{18}O$ molecules would take more than 4 times longer to diffuse out of the soil than it would take them to re-equilibrate with soil water. However, whilst use of this setting-point is a convenient approximation in field settings (Wingate et al., 2009, 2010), some degree of exchange still occurs above this depth (Kapiluto et al., 2007). Given the need to make an assumption about

10   the soil water pool with which CO_2 is interacting, the potential for spatial and temporal variability of δ_{sw}, and limited *a priori* information with respect to appropriate sampling resolution and depth (Miller et al., 1999; Riley, 2005), approaches allowing CA activity to be estimated in the absence of this information are desirable.

Here we test whether soil CA activity can be reasonably estimated in the absence of independent information about δ_{sw} and

15   investigate assumptions about soil CO_2-H_2O isotope equilibration. To do so we apply a novel approach to obtain solutions for v_{inv} and δ_{eq}, as a function of the response of δ_R to variations in δ_a, from gas flux measurements. Equation 1 describes a linear relationship of the form $\delta_R = m\delta_a + c$, where the slope, m, is $-v_{inv}C_a/F_R$ and the intercept, c, is $v_{inv}C_a/F_R\ \delta_{eq} + \delta_{eq} - a$. If C_a and F_R are held constant, v_{inv} and δ_{eq} can be estimated from a linear regression between δ_R and δ_a:

$$v_{inv} = \frac{-m}{C_a/F_R} \text{,}$$

(3a)

$$\delta_{eq} = \frac{c+a}{1-m}$$

(3b)

To test this approach, we conducted laboratory incubations using air-dried soils that were irrigated with one of three different waters that differed in terms of their $\delta^{18}O$ ($\delta_{iw,low}$, $\delta_{iw,med}$ or $\delta_{iw,high}$). The gas fluxes from these incubations were then sequentially measured under three different inlet conditions that varied in terms of the $\delta^{18}O$ of CO_2 ($\delta_{b,low}$, $\delta_{b,med}$ and $\delta_{b,high}$) but

25   not in terms of total CO_2 concentration (C_b). Following gas measurements, water was cryogenically extracted from the incubated soils and its isotopic composition determined ($\delta_{sw,ce}$) to allow for comparison with that estimated to be in equilibrium with CO_2 from the gas flux measurements ($\delta_{sw,eq}$). We specifically aimed to 1) confirm the suitability of this approach by testing whether δ_R and δ_a are linearly related in an experimental context, 2) compare estimates of $\delta_{sw,eq}$ determined from the gas flux measurements with $\delta_{sw,ce}$ measured for the extracted bulk soil water, and 3) compare the

30   sensitivity of k_{iso} estimates to variations in δ_{sw}.

2 Materials and methods

2.1 Soil sampling and incubation preparation

Soil was collected in April, 2016 from Le Bray, a *Pinus pinaster* plantation in the southwest of France with predominately sandy soil (87.4 % coarse sand, 6.2 % fine sand, 2.7 % silt and 3.7 % clay), 3 % organic carbon and a water-holding capacity

5   of 0.27 g g^{-1} (Ogée et al., 2004; Wingate et al., 2010). After the removal of the under-story and the litter layer, consisting of living and dead *Molinia caerulea* tussocks, pine needles, pine cones, and wood fragments, about 6 kg of soil was collected from the superficial 10 cm at 4 locations spaced 5 m apart. This material was mixed and passed through a 4 mm sieve to remove any large debris. Three sub-samples of the sieved soil were taken to determine the pH, water content and $\delta_{sw,ce}$ of the fresh, sieved soil. The soil was air-dried for approximately two weeks before being stored in a closed box containing

10 desiccant until the incubations were conducted between mid-June and mid-August, 2016. Approximately 400 g of soil was used to determine the $\delta_{sw,ce}$ of any residual soil water and 6 sub-samples were taken to determine pH after drying.

A total of 18 incubations were conducted with 6 replicates for each level of the irrigation water treatment. Each incubation was prepared by placing about 430 g of air-dried soil in a plastic zip lock bag. Approximately 30 g of soil were removed to

15 determine the residual water content and the remaining 400 g were re-wetted inside the bag with 40 ml of $\delta_{iw,low}$, $\delta_{iw,med}$ or $\delta_{iw,high}$ irrigation water. The bag was closed, gently mixed by hand and 300 g of wet soil was then placed into a threaded polytetrafluoroethylene chamber with a height of 11.6 cm and an internal diameter of 7.3 cm. The chamber was closed with a screw-top polytetrafluoroethylene lid and shaken at 200 rpm for 10 minutes on an orbital shaker. The remaining 100 g of wet soil in the bag was then sampled for determination of the re-wetted water content and the initial $\delta_{sw,ce}$. Following shaking, the

20 chamber was opened, sharply tapped to encourage the soil to settle in a uniform manner and placed inside a humidifier designed to maintain the soil water content and composition prior to the gas exchange measurements. This consisted of a desiccator filled with 500 ml of the irrigation water through which ambient air was bubbled using a membrane pump. The humidifier was wrapped in reflective foil and kept in a temperature controlled room at 21 °C. Relative humidity and temperature inside the humidifier were monitored using a small combined sensor and data-logger (Hydrochron, iButtonLink,

25 LLC., USA).

Typically, preparation and pre-incubation of the soils for each level of the water treatment spanned 3 days. Three chambers, staggered at 2 hour intervals, were prepared on each of the first two days. The water used to re-wet the soil and initially fill the humidifier was sampled at the start of each day to characterise the isotopic composition of $\delta_{iw,low}$, $\delta_{iw,med}$ and $\delta_{iw,high}$. The

30 water in the humidifier was sampled once on day 2 and twice on day 3 to track any change in its isotopic composition over the course of the pre-incubation (not shown). Each chamber was pre-incubated for 24 hours and then removed from the

humidifier, weighed to determine water loss and finally connected to the gas exchange system. Following gas exchange measurements, the chamber was immediately removed, and re-weighed to determine water loss over the measurement period. The depth of the soil (z_{max}) inside the chamber was then measured at 4 points using a digital calliper, and 1cm-thick horizons, from 0 to 5 cm depth, removed and split for determination of depth-resolved water content and $\delta_{sw,ce}$.

Gravimetric water content was determined from weight change after oven drying at 105 °C for 24 hours. Soil pH was determined from a soil-to-water slurry of 1:5 and measured in the supernatant after 2 hours. Soil bulk density was calculated from the initial gravimetric water content after re-wetting, the wet weight of the soil in the chamber and the volume of the soil in the chamber. Total porosity (ϕ_t) was calculated from bulk density assuming a particle density of 2.65 g cm^{-3} (Linn and Doran, 1984). Volumetric water content (θ_w) was calculated as the product of gravimetric water content and bulk density and ϕ_a as the difference between ϕ_t and θ_w.

2.2 Soil water extraction and analysis

Soil samples taken for determination of $\delta_{sw,ce}$ consisted of 20 to 25 g of material stored at 4 °C in 20 ml glass vials with positive insert screw-top caps. Water samples were extracted from these soils using a cryogenic vacuum distillation system based on the design and methodology described by Orlowski et al. (2013). In brief, the system consists of 6 branches each equipped with 4 extraction vessels, a pirani vacuum gauge (APG100-XLC, Edwards, UK) and an isolation valve. The branches connect to a manifold equipped with a vacuum gauge, a vacuum release valve and a two-stage rotary vane vacuum pump (RV5, Edwards, UK). Extractions were prepared by placing about 20 g of soil, topped with oven-baked glass wool, into an extraction vessel. For each branch, extraction vessels were weighed and frozen in a bath of liquid nitrogen. After freezing, the manifold and branches were checked for leaks using the vacuum gauges and evacuated to a starting pressure of less than 0.3 Pa. Extractions were initiated by isolating a branch, transferring the liquid nitrogen bath to a U-shaped water trap and the sample vessels to a water bath initially at room temperature. Extractions lasted for 180 minutes and the water bath was set to 80 °C after 60 minutes. Following extraction, the water traps were removed, the ends sealed with parafilm and the collected ice allowed to thaw before being weighed. The extracted waters were transferred to 5 ml glass vials with positive insert screw-top caps and stored at 4 °C. Extraction vessels and empty water traps were oven-dried and re-weighed to determine extraction efficiency.

The accuracy of cryogenic vacuum distillation techniques has been questioned as the $\delta^{18}O$ of extracted waters tend to be depleted in ^{18}O, the extent of which depending on soil properties, relative to the irrigation water when oven dried soils that have been re-wetted are considered (Orlowski et al., 2016a; Sprenger et al., 2015). To quantify biases associated with our methodology and the soil studied, two tests were conducted where six 20 g soil samples were re-wetted to a gravimetric

water content of about 0.1 g g^{-1} with water that had a δ^{18}O of -4.84 ± 0.06 ‰ Vienna Standard Mean Ocean Water-Standard Light Antarctic Precipitation (VSMOW-SLAP). In the first test, residual water was removed from air-dried soil by oven drying at 105 °C for 24 hours prior to re-wetting. In the second test, residual water was removed by cryogenic extraction following the above methodology prior to re-wetting. These soils were then treated as described for samples.

The δ^{18}O of the irrigation waters, $\delta_{iw,low}$, $\delta_{iw,med}$ and $\delta_{iw,high}$, and cryogenically extracted water samples, $\delta_{sw,ce}$, were measured on an off-axis integrated cavity optical spectrometer (TIWA-45EP, Los Gatos Research, USA) coupled to an auto-sampler (Berman et al., 2013). Prior to analysis, 1 ml of each water sample was pipetted into a 1.5 ml vial and capped with a pre-slit septa. An auto-sampler equipped with a 5 µl syringe and a heated septum port (PAL LC-xt, CTC Analytics AG, Switzerland) sequentially injected 8 aliquots of each sample into the analyser. The first three injections for each sample were discarded to avoid inter-sample memory effects (Lis et al., 2008), as were any injections flagged by the analyser's software (Berman et al., 2013). To avoid applying a linearity correction, the mean water density for a run was calculated and any injection with a water density more than 10^{15} molecules cm^{-3} away from the mean was rejected (Lis et al., 2008). The mean water density was then re-calculated and only injections within three standard deviations were retained. A raw mean δ^{18}O was calculated for all samples where 3 to 5 injections were retained. We accounted for analyser drift and report on the VSMOW-SLAP scale by including two working standards (-10.31 ‰ and 0.62 ‰ VSMOW-SLAP) and a quality control sample (-4.84 ± 0.06 ‰ VSMOW-SLAP) between every 5 unknown samples.

2.3 Incubation system and gas analysis

Measurement of gas fluxes under the three different inlet conditions, $\delta_{b,low}$, $\delta_{b,med}$ and $\delta_{b,high}$, was achieved using a gas supply manifold capable of delivering one of three gas mixtures to the inlet of the incubation system (Fig. 1). Briefly, the inlet to the incubation system was connected to a normally closed 2/2 solenoid valve actuated by a micro-controller (Arduino Uno, Arduino LLC, Italy). One port of the valve was connected directly to a cylinder of compressed air ($\delta_{b,high}$) with a total CO_2 concentration and δ^{18}O of 424.93 ± 0.01 ppm and -3.45 ± 0.02 ‰ VPDB$_g$ (NOAA Earth System Research Laboratory, USA). The other ports were preceded by open splits and connected to continuous flows from two in-house gas dilution systems capable of providing a given concentration of CO_2 by mixing pure CO_2 from gas cylinders into CO_2-free air generated by an air compressor (FM2 Atlas Copto, Nacka, Sweden) equipped with a scrubbing column (Ecodry K-MT6, Parker Hannifin, USA). The concentrations of the two gas dilutions were adjusted to match that of the cylinder containing $\delta_{b,high}$ and contrasts in δ^{18}O were achieved by using pure CO_2 cylinders of different origins ($\delta_{b,med}$ and $\delta_{b,low}$). Following the inlet of the incubation system, the gas stream was split into a chamber and bypass line that terminated at open splits in front of a normally closed 2/2 solenoid valve connected to the sample inlet of a CO_2 isotope ratio infra-red spectrometer (DeltaRay IRIS, Thermo

Fischer Scientific, Germany). The flow rate of each line was limited to 216 ml min^{-1} using two mass-flow controllers. The soil chamber was connected in-line at the middle of the chamber line and placed in a water bath at 21 °C.

Gas exchange measurements were made by alternately switching the valve to the sample inlet of the IRIS, allowing approximately 80 ml min^{-1} of the total flow to pass through the instrument, between bypass and chamber lines three times. The IRIS reports concentrations at 1 Hz for the three most abundant isotopologues of CO_2 ($^{12}C^{16}O^{16}O$, $^{13}C^{16}O^{16}O$ and $^{12}C^{18}O^{16}O$), allowing determination of the total concentration and isotopic composition of CO_2 (Geldern et al., 2014; Rizzo et al., 2014). The stability of measurements of the total concentration and the $\delta^{18}O$ of CO_2 were assessed prior to the gas exchange measurements by analysing the contents of an air cylinder for 22.5 h (Fig. S1) and subsequent computation of Allan variances (Carrio, 2015). A maximum precision of 0.01 ppm for total CO_2 and 0.05 ‰ VPDB$_g$ for $\delta^{18}O$ was achieved after integrating over 172 s and 144 s, respectively. Given the profile of the Allan plot (Werle, 2010) and the 35 s residence time of the air in the instrument cell (Geldern et al., 2014), a measurement period of 120 s was used. The first 80 s of each measurement were discarded to minimise carry-over effects and the final 40 s were kept and averaged to provide a measurement mean and standard deviation. A 40 s integration period corresponds to standard deviations for total CO_2 and the $\delta^{18}O$ of CO_2 of 0.02 ppm and 0.06 ‰ VPDB$_g$, respectively. Averaged isotopologue concentrations were corrected by bracketing every three pairs of bypass and chamber line measurements with the measurement of two calibration cylinders (Deuste Steinger GmbH, Germany). The standard deviations for total CO_2 and the $\delta^{18}O$ of CO_2 over 960 s (the interval between two calibration measurements) were 0.02 ppm and 0.06 ‰ VPDB$_g$, respectively.

The calibration cylinders contained mixtures of CO_2 in synthetic air (21% O_2 and 0.93% Ar in a N_2 balance) that had been characterised for the total concentration, carbon isotope composition and $\delta^{18}O$ of CO_2 (Max Planck Institute for Biogeochemistry IsoLab, Germany). The total concentration, carbon isotope composition and $\delta^{18}O$ of CO_2 for each cylinder were, respectively, 380.26 ppm, -3.064 ‰ VPDB and -14.631 ‰ VPDB$_g$, and 481.62 ppm, -3.071 ‰ VPDB and -14.698 ‰ VPDB$_g$. Concentrations of $^{12}C^{16}O^{16}O$, $^{13}C^{16}O^{16}O$ and $^{12}C^{18}O^{16}O$ were calculated from these values following Wen et al. (2013). Measured averages for the calibration cylinders were linearly interpolated and correction coefficients calculated from two-point linear regressions between cylinders, allowing correction of sample isotopologue concentrations and calculation of total concentration and $\delta^{18}O$ of CO_2 (Bowling et al., 2003; Wen et al., 2013; Wingate et al., 2010). This calibration scheme was validated for our isotopic measurements by allowing 40 l of pure CO_2 to equilibrate with 4 l of water in a 25 l barrel at 24 °C. Approximately three months after filling, the $\delta^{18}O$ of CO_2, calibrated using the scheme described above, in the barrel head-space was measured in dilutions with concentrations ranging from 390 to 560 ppm. Following these measurements the water with which the CO_2 had equilibrated with was sampled and its $\delta^{18}O$ determined as described previously. Measurements of $\delta^{18}O$ of CO_2 were not significantly dependent on CO_2 concentration over this range but the

composition of the $\delta^{18}O$ of CO_2 was, on average, 0.31 ‰ more depleted than that of the water. To account for this offset between our gas and water measurements, a post-calibration correction of +0.31 ‰ was applied to all bypass and chamber CO_2 measurements.

5   The net soil CO_2 flux, F_R, was calculated from the corrected values for each pair of calibrated bypass and chamber measurements as:

$$F_R = \frac{u}{A}(C_a - C_b)$$

$$,\tag{5}$$

where u (mol s^{-1}) is the flow rate of dry air through the chamber line, C_a (ppm) is the CO_2 concentration of the chamber line, C_b (ppm) is the CO_2 concentration of the bypass line, and A (m^2) is the surface area of the soil in the chamber. Similarly, the

10    $\delta^{18}O$ of soil-atmosphere CO_2 exchange, δ_R, was calculated as:

$$\delta_R = \frac{\delta_a C_{a,12} - \delta_b C_{b,12}}{C_{a,12} - C_{b,12}}$$

$$,\tag{6}$$

where δ_a and $C_{a,12}$ (ppm) are respectively the $\delta^{18}O$ of CO_2 and concentration of $^{12}C^{16}O^{16}O$ in the chamber line and δ_b and $C_{b,12}$ (ppm) are the $\delta^{18}O$ of CO_2 and concentration of $^{12}C^{16}O^{16}O$ in the bypass line. To ensure steady-state conditions for measurements under the three different inlet conditions, a complete cycle where only the chamber line was measured was

15   included to allow the chamber head-space and soil pore-space conditions to stabilise between transitions from atmospheric conditions at the start of the incubation and subsequent inlet conditions (Fig. 2). The order of the inlet conditions was varied between the 6 replicates of each level of the irrigation water treatment to avoid introducing a temporal measurement bias.

2.4 Data processing

All data processing and analysis was conducted in R version 3.3 (R Core Team, 2017). The slopes and intercepts of linear

20   relationships between the $\delta^{18}O$ of soil-atmosphere CO_2 exchange, δ_R, and the $\delta^{18}O$ of CO_2 at the soil surface (taken here to be that of the chamber line), δ_a, were calculated from the measurements made under the three different inlet conditions for each of the incubations (Bates et al., 2015). Following Eq. 3a, the piston velocity of CO_2, v_{inv}, was estimated using the slope of the linear regression, m, and the mean ratio of concentration of CO_2 at the soil surface and net CO_2 flux, C_a/F_R, for each incubation. As Eq. 3 is only strictly valid when there is a semi-infinite soil column (Tans, 1998), we adapted the equation to

25   account for the influence of boundary conditions found at the bottom of the incubation vessel. The soil-depth adjusted piston velocity ($\tilde{v}_{inv}$), was estimated by using v_{inv} obtained from Eq. 3a to iteratively satisfy:

$$v_{inv} = \tilde{v}_{inv} \tanh\left(\frac{\tilde{v}_{inv} z_{max}}{\kappa \phi_a D}\right)$$

$$,\tag{7}$$

where z_{max} (m) is the total soil column depth. In doing so we adopted the formulation of Moldrup et al. (2003) for the tortuosity, κ, of repacked soils:

$$\kappa = \frac{\phi_a^{1.5}}{\phi_t}$$

(8)

Temperature-dependant CO_2 solubility, B, was calculated using Weiss (1974) and the diffusivity of $^{12}C^{16}O^{18}O$ in air, D, was calculated according to Massman (1998) and Tans (1998):

$$D = 1.381\,e^{-5}\frac{T}{273.15}^{1.81}\left(1-\frac{a}{1000}\right),$$

(9)

where T (K) is soil temperature. Derived estimates of $\tilde{v}_{inv}$ were then used to calculate the apparent rate of hydration, k_{iso}, by replacing v_{inv} with $\tilde{v}_{inv}$ in Eq. 2. The difference between the semi-infinite and finite-depth solutions are shown in Fig. S2 for different soil depths. For this soil type and water content, a soil depth of > 8 cm is necessary to be able to neglect the influence of boundary conditions found at the bottom of the incubation vessel.

Corrections for a finite soil depth had also to be applied to estimate, the $\delta^{18}O$ of CO_2 in equilibrium with soil water, δ_{eq}. For this, the soil-depth adjusted isotopic fractionation associated with the diffusion of CO_2 ($\tilde{a}$) was first calculated as:

$$\tilde{a} = a\left(1 - \frac{\kappa\phi_a D}{\tilde{v}_{inv} z_{max}}\tanh\left(\frac{\tilde{v}_{inv} z_{max}}{\kappa\phi_a D}\right)\right),$$

(10)

where the full diffusional fractionation, a, was set to 8.8 ‰ (Riley, 2005). Estimates of δ_{eq} were then obtained using the intercept, c, of the linear regression and by replacing the slope, m, with $-\tilde{v}_{inv}C_a/F_R$ and a with $\tilde{a}$ in Eq. 3b. To allow for comparison with the $\delta^{18}O$ of soil water determined following cryogenic extraction, $\delta_{sw,ce}$, derived estimates of δ_{eq} were converted to equivalent values of the $\delta^{18}O$ of soil water in equilibrium with CO_2, $\delta_{sw,eq}$, based on the temperature-dependant equilibration fractionation between water and CO_2 and the difference between the VPDB$_g$ and VSMOW-SLAP scales (Brenninkmeijer et al., 1983; Kapiluto et al., 2007; Wingate et al., 2010):

$$\delta_{sw,eq} = \delta_{eq} + 0.2(T - 297.15)$$

(11)

Treatment summaries are reported as mean and standard deviation unless stated otherwise. A total of 18 incubations were conducted on sub-samples of same homogenised soil. Six independently replicated incubations were conducted for each level ($\delta_{iw,low}$, $\delta_{iw,med}$ and $\delta_{iw,high}$) of the irrigation water treatment. Soil properties and model parameters were determined individually for each incubation as described above. Differences in soil properties and model parameters in response to the

water treatment, with statistical significance reported at p < 0.01, were tested through one-way analysis of variance with post-hoc comparison by Tukey's HSD (Crawley, 2007; Mendiburu, 2016). To do so, a given property or parameter was taken as the dependent variable and water treatment as the categorical independent variable.

3 Results

3.1 Soil properties

The gravimetric water content and pH of freshly sampled, sieved soil was 0.207 ± 0.005 g g^{-1} and 4.75 ± 0.05 respectively. The pH of the air-dried soil was 4.34 ± 0.02. Measured soil properties were not statistically different among water treatments. Following drying and storage, the gravimetric water content of air-dried soil measured during incubation preparation was 0.010 ± 0.001 g g^{-1}. After re-wetting and mixing, the gravimetric water content of the soil placed into incubation chambers was 0.107 ± 0.002 g g^{-1}. During the 24-hour pre-incubation 0.172 ± 0.075 g of water evaporated and a further 0.361 ± 0.050 g of water was subsequently lost over the course of the 96 min gas exchange measurement. Gravimetric water contents were 0.099 ± 0.005 g g^{-1} at 0–1 cm, 0.105 ± 0.003 g g^{-1} at 1–2 cm, 0.106 ± 0.003 g g^{-1} at 2–3 cm, 0.107 ± 0.003 g g^{-1} at 3–4 cm, and 0.107 ± 0.002 g g^{-1} at 4–5 cm. The other soil properties determined following gas exchange measurements are summarised by water treatment in Table 1.

3.2 Water composition

The δ^{18}O of soil water determined following cryogenic extraction, $\delta_{sw,ce}$, of freshly sampled soil was -3.63 ± 0.10 ‰ VSMOW-SLAP. After air drying and storage, the $\delta_{sw,ce}$ of the residual water pool was -6.69 ± 0.01 ‰ VSMOW-SLAP. Mean δ^{18}O and standard errors for the $\delta_{iw,low}$, $\delta_{iw,med}$ and $\delta_{iw,high}$ irrigation waters were respectively -6.74 ± 0.03, -3.69 ± 0.03 and 0.24 ± 0.04 ‰ VSMOW-SLAP. The addition of these waters to the air-dried soils used in the incubations resulted in initial $\delta_{sw,ce}$ of -7.03 ± 0.34, -4.28 ± 0.21 and -0.80 ± 0.05 ‰ VSMOW-SLAP for the $\delta_{iw,low}$, $\delta_{iw,med}$ and $\delta_{iw,high}$ treatments, respectively. The difference between the composition of the irrigation water and the initial $\delta_{sw,ce}$ was 0.29 ± 0.35 ‰ VSMOW-SLAP for the $\delta_{iw,low}$ treatment, 0.58 ± 0.22 ‰ VSMOW-SLAP for the $\delta_{iw,med}$ treatment and 1.04 ± 0.05 ‰ VSMOW-SLAP for the $\delta_{iw,high}$ treatment. Evaporation during pre-incubation and gas measurements (Fig. 3) resulted in final $\delta_{sw,ce}$ (averaged between 0 and 5 cm depth and weighted by water content) of -6.75 ± 0.11, -4.17 ± 0.36 and -0.55 ± 0.07 ‰ VSMOW-SLAP for the $\delta_{iw,low}$, $\delta_{iw,med}$ and $\delta_{iw,high}$ treatments, respectively.

The $\delta_{sw,ce}$ of the methodological tests using soil where residual water was removed prior to labelling by oven drying was -5.41 ± 0.19 ‰ VSMOW-SLAP, i.e. 0.57 ‰ more depleted than the labelling water. Similarly, the δ_{sw-ce} of the soil where

residual water was removed by cryogenic extraction ($n = 5$) was -5.01 ± 0.18 ‰ VSMOW-SLAP and overlapped with the labelling water with a mean depletion of only 0.17 ‰.

3.3 Gas measurements

The mean CO_2 concentration, C_b, of the three different inlet gases ($\delta_{b,low}$, $\delta_{b,med}$, and $\delta_{b,high}$) measured in the bypass line were between 422 and 426 ppm for all water treatments, with standard deviations for individual gas mixtures and water treatments smaller than 2 ppm (Table 2). The mean CO_2 concentration, C_a, measured in the chamber line for these inlet conditions varied between 480 and 497 ppm, with standard deviations for individual gas mixtures and water treatments between 2 and 15 ppm (Table 2). Subsequently, the resultant mean of CO_2 fluxes, F_R (Eq. 5), for $\delta_{b,low}$, $\delta_{b,med}$, and $\delta_{b,high}$ were 1.98 ± 0.01 μmol m^{-2} s^{-1} for the $\delta_{iw,low}$ treatment, 2.51 ± 0.01 μmol m^{-2} s^{-1} for the $\delta_{iw,med}$ treatment and 2.22 ± 0.01 μmol m^{-2} s^{-1} for the $\delta_{iw,high}$ treatment, with standard deviations for individual gas mixtures and water treatments between 0.1 and 0.6 μmol m^{-2} s^{-1}. The similarity within water treatment demonstrates the good repeatability of the experiment, however, the greater variability in C_a compared to C_b indicates that steady-state conditions may not have always been fully attained (the order of inlet conditions was varied among incubations). Indeed, whilst there was no general relationship between F_R and C_b, F_R linearly decreased with time ($r^2 = 0.83$ to 0.99), at a rate between 0.078 to 0.31 μmol m^{-2} h^{-1} over the course of all the incubations. Because of these trends, incubation mean ratios of C_a/F_R were 10200 ± 1200, 8350 ± 1100 and 9140 ± 320 s m^{-1} for the $\delta_{iw,low}$, $\delta_{iw,med}$, and $\delta_{iw,high}$ treatments, respectively. Standard deviations associated with the ratio for individual incubations were between 240 and 425 s m^{-1}.

Mean $\delta^{18}O$ of CO_2 in the bypass, δ_b, and chamber, δ_a, lines for the different water treatments and inlet conditions are given in Table 2 together with the resultant exchange, δ_R (Eq. 6). Unlike F_R there was no general relationship between δ_R and time but, as expected, δ_R was strongly negatively correlated with δ_b ($r^2 > 0.95$ in all the incubations). Generally variability in these measurements was largest for the $\delta_{b,low}$ gas mixture.

3.4 Estimates of k_{iso} and $\delta_{sw,eq}$

In all the incubations δ_a and δ_R were strongly ($r^2 > 0.93$) and negatively correlated (Fig. 4). The slope, m, of the linear regressions were broadly similar among water treatments with means of -1.83 ± 0.25 for the $\delta_{iw,low}$ treatment, -1.32 ± 0.25 for the $\delta_{iw,med}$ treatment, and -1.53 ± 0.15 for the $\delta_{iw,high}$ treatment. In contrast, the intercept, c, of the linear regressions between δ_a and δ_R were more distinct with treatment means of -30.17 ± 2.14 ‰ VPDB$_g$ for the $\delta_{iw,low}$ treatment, -20.08 ± 2.66 ‰ VPDB$_g$ for the $\delta_{iw,med}$ treatment and -14.29 ± 1.21 ‰ VPDB$_g$ for the $\delta_{iw,high}$ treatment.

The mean piston velocity assuming a semi-infinite soil column, v_{inv} (Eq. 3a), varied between 0.16 and 0.18 mm s^{-1} (Table 3). Accounting for the finite depth of the soil column lead to $\tilde{v}_{inv}$ values (Eq. 7) that were systematically but only marginally larger (Table 3), mostly because soil depth, z_{max}, had been chosen to minimise this difference (Table 1 and Fig. S2). These values led to CO_2-H_2O isotopic exchange rates, k_{iso}, that were not significantly different between treatments (Table 3).

Estimates of the effective fractionation, $\tilde{a}$ (Eq. 10), were approximately half the full fractionation of 8.8 ‰ (Table 3). Expectedly, estimated values of the isotopic composition of CO_2 in equilibrium with soil water, δ_{eq} (Eq. 3b), were significantly different among water treatments. These values led to equivalent values of the isotopic composition of soil water in equilibrium with CO_2, $\delta_{sw,eq}$ (Eq. 11), that were also significantly different between treatments (Table 3), and surprisingly more depleted than the isotopic composition of cryogenically extracted soil water, $\delta_{sw,ce}$, at all depths (Fig. 3).

4 Discussion

Our first aim was to confirm the assumption that the isotopic compositions of the CO_2 flux, δ_R, and the CO_2 of the air at the soil-air interface, δ_a, are linearly related (Eq. 1). This appears to be a good approximation for our data with strong correlations between δ_R and δ_a in all experiments (Fig. 4). However, a number of other assumptions inherent to applying the model described by Eq. 1 in this way may influence our results. Namely, that CO_2 production profiles were constant with depth and that gas flux measurements were made under steady-state conditions (Tans, 1998). The first point is unlikely to be an issue here because care was taken to homogenise the soils before each gas exchange measurement (see Methods) and the total period between preparation and measurement (24 hr) was too short to allow large gradients, for example in soil moisture, that might cause an unequal respiration profile to develop. Potential deviations from steady-state conditions require more attention. A period of 21 min was included before the measurements from which fluxes were calculated, not only at the initial connection of an incubation chamber but also after each subsequent switch of the inlet conditions (Fig. 2). This period was chosen based on initial tests indicating that 10 min was sufficient for the concentration and composition of CO_2 to stabilise in an empty chamber and calculations indicating that full isotopic equilibrium of the CO_2-H_2O system, given the acidity and temperature of the soil, should theoretically be reached within 12 minutes even at un-catalysed rates (Uchikawa and Zeebe, 2012). However, our results showed that the net soil CO_2 flux, F_R, systematically decreased with time by about 10 % on average between the first and last measurements within an incubation. This indicates that our measurements did not strictly adhere to the assumption of steady state. This trend probably reflects a combination of dissolved CO_2 de-gassing from the soil water as a result of small differences between pre-incubation and incubation CO_2 concentrations and, probably more importantly, the temporal response of soil respiration to re-wetting (Birch, 1958; Jarvis et al., 2007). As such, the ratio between the concentration of CO_2 at the soil surface, C_a, and F_R is not strictly constant and this introduces uncertainties into

the estimations of the apparent rate of exchange, k_{iso}, and the isotopic composition of soil water, $\delta_{sw\text{-}eq}$, that are considerably larger than that associated with individual gas measurements. Indeed, propagating this within-incubation variability in the ratio of C_a/F_R leads to within-incubation uncertainties in k_{iso} of around 0.01 s^{-1} for all treatments and within-incubation uncertainties in $\delta_{sw\text{-}eq}$ of 0.45, 0.37 and 0.24 ‰ for the $\delta_{iw,low}$, $\delta_{iw,med}$ and $\delta_{iw,high}$ treatments. These within-incubation
5   uncertainties are the same of order magnitude as the variability in treatment means (Table 3), indicating that this temporal deviation from steady-state conditions may be the cause of much of the reported variability. This variability could be reduced in future studies by working with fresh soils or allowing longer acclimatisation periods after re-wetting, provided efforts are made to limit the development of heterogeneity in the soil profile. As the linearity between δ_R and δ_a appears strong, variability could also be reduced by considering two rather than three inlet conditions to shorten the overall measurement
10   time.

Secondly, we aimed to compare estimates of $\delta_{sw,eq}$ determined from the gas flux measurements with $\delta_{sw,ce}$ measured for the extracted bulk soil water. Given the relatively constant profile of $\delta_{sw,ce}$ with depth (Fig 3) and the fact that total soil depth, z_{max}, was shallower than that required for full convergence between the semi-infinite and finite soil depth model solutions (Table
15   3, Fig S2), the estimates of $\delta_{sw,eq}$ reported likely reflect interaction between CO_2 and soil water across the total soil depth (Kapiluto et al., 2007). Whilst $\delta_{sw,eq}$ estimates were distinct among water treatments, they were also consistently more depleted than $\delta_{sw,ce}$ with mean offsets from $\delta_{sw,ce}$ between 0 and 5 cm of -2.56 ± 0.11, -2.87 ± 0.56 and -3.61 ± 0.23 ‰ VSMOW-SLAP for the $\delta_{iw,low}$, $\delta_{iw,med}$, and $\delta_{iw,high}$ treatments, respectively. Given the difference between the externally assigned value of -3.45 ± 0.02 ‰ VPDB$_g$ for the gas cylinder used as the $\delta_{b,high}$ inlet condition and its measurement, with treatment
20   means of -3.63 ± 0.15, -3.62 ± 0.3 and -3.58 ± 0.11 ‰ VPDB$_g$ for $\delta_{iw,low}$, $\delta_{iw,med}$, and $\delta_{iw,high}$ respectively, we find no evidence that an offset between the calibration of our gas and water measurement scales could account for the size of the offset observed. Similarly, we find no evidence for large biases in our cryogenic extraction methodology as $\delta_{sw,ce}$ and composition of the labelling water overlapped in the tests where residual water was removed under extraction conditions prior to label addition (Orlowski et al., 2013, 2016b) . This suggests that the offset between $\delta_{sw,eq}$ and $\delta_{sw,ce}$ is the result of CO_2 interacting
25   with a water pool whose isotopic composition is more depleted than $\delta_{sw,ce}$. Differences in the water pools characterised by different methodologies for determining the isotopic composition of soil waters are well known, with the cryogenic extraction method being expected to remove macro-pore, micro-pore, hygroscopic and potentially crystalline water, whilst the static equilibration of soils with CO_2 is expected to principally reflect only the macro-pore and micro-pore pools (Hsieh et al., 1998b; Orlowski et al., 2016b; Sprenger et al., 2015). For this reason, we might expect $\delta_{sw,eq}$ derived here to reflect the
30   isotopic composition of macro-pore and micro-pore pools and $\delta_{sw,ce}$ to reflect both these as well as hygroscopic and crystalline waters. However, disregarding the crystalline water pool in this predominately sandy soil, this would suggest that the isotopic composition of the hygroscopic pool would have to be considerably more positive than that of the macro-pore

and micro-pore water pools in order to account for the fact that $\delta_{sw,eq}$ estimates were more negative than $\delta_{sw,ce}$. Contrary to this, extraction of water from the air-dried soil, of which hygroscopic water presumably represents a greater portion of the total water pool than in re-wetted samples, yielded a $\delta_{sw,ce}$ more depleted than that of the freshly sampled soil and the initial compositions of both the $\delta_{iw,med}$, and $\delta_{iw,high}$ treatments. This suggests that this residual pool in fact reflects the potentially

5   rapid and dynamic exchange with atmospheric vapour during storage (Lin and Horita, 2016; Orlowski et al., 2016b; Savin and Epstein, 1970). Indeed, the fact that about 10 % of water in the re-wetted soils consisted of this residual pool helps account for the differences between the composition of the added water and initial δ_{sw-ce} across the water treatments. Observations that fractionation occurs between water associated with, cations and anions present in solution or at mineral surfaces (Oerter et al., 2014), organic particle surfaces (Chen et al., 2016), and pore surfaces (Lin and Horita, 2016) and bulk

10   water pools may help explain our data. In particular, Chen et al. (2016) found that the composition of the water bound to organic particle surfaces could be up to 4 ‰ more depleted than bulk water, with a greater fractionation at higher volumetric ratios of solid to water. Such a depletion in bound (hygroscopic) water would explain our data, given the relatively low water content of the soil studied. However this requires us to consider that CO_2 is being heavily influenced by exchange with hygroscopic water under our experimental conditions. Such interaction between CO_2 and hygroscopic water may be

15   plausible as surface water films are where microbial communities expressing CA are likely to be present and active. If interaction with hygroscopic water were the cause of this observation, we should expect to see a smaller offset between $\delta_{sw,eq}$ and $\delta_{sw,ce}$ at higher water content because, as water content increases, so does the proportion of non-hygroscopic to hygroscopic water that CO_2 interacts with during the slow process of liquid phase diffusion (4 orders of magnitude lower than gas phase diffusion). We estimated that, even at the uncatalysed rate of hydration, CO_2 molecules would be fully

20   equilibrated if they had to diffuse through about 0.5 mm of water. Whilst this is not realistic for water films adsorbed onto pore-surfaces, such path-lengths are plausible for filled capillaries as the soil-pore network approaches saturation (Lebeau and Konrad, 2010; Tokunaga, 2011; Tuller and Or, 2001). We tested this by creating and measuring an additional six incubations, following the methods described above, that were re-wetted with different amounts of the same water to achieve water contents ranging from about 15 to 70 % water-filled pore space. The difference between estimated $\delta_{sw,eq}$ and $\delta_{sw,ce}$

25   determined for sampling depths of 0-1 cm ($r^2 = 0.92$) and 1-5 cm ($r^2 = 0.88$) were positively and linearly correlated with water-filled pored space across these incubations (Fig. 5). The fact that these relationships indicate the offset decreases at higher water contents may indeed support the inference that estimates of $\delta_{sw,eq}$ are being influenced by fractionation between surface and bulk water pools in our measurements.

30   Finally, we aimed to compare the sensitivity of estimates of k_{iso} to δ_{sw}. Estimates of k_{iso} ranged from 6.8 to 14.6 times greater than the theoretical un-catalysed rate of CO_2-H_2O isotopic exchange of 0.006 s^{-1} for the incubation conditions (Uchikawa and Zeebe, 2012). This enhancement of the apparent over the un-catalysed rate of hydration indicates that the reaction is indeed

being catalysed by the presence of CA in these soils. After considering differences in the value of un-catalysed rate of CO_2-H_2O exchange used, these rates are on the lower end of those reported from soil chambers deployed in the forest where soil used here was collected (Wingate et al., 2009; Wingate et al., 2010). Our estimates of k_{iso} were not distinct among water treatments (Table 3), supporting the idea that our new approach is robust enough to assay soil CA activity in the absence of
5 information about δ_{sw}. This is beneficial as this approach also does not rely on any assumption about which soil water pool the CO_2 must equilibrate with, as such an assumption could introduce strong biases in the retrieved k_{iso}. To illustrate this point, we compared our new approach with previous studies (Wingate et al., 2009, 2008) where δ_{sw} has been used to determine k_{iso} from Eq. 1 and Eq. 2. For this, we replaced v_{inv} and a in these equations with $\tilde{v}_{inv}$ (Eq. 7) and $\tilde{a}$ (Eq. 10) and iteratively solved for $\tilde{v}_{inv}$ using $\delta_{sw,ce}$ and gas measurements made at the individual inlet conditions reported here. In doing so
10 we highlight the potential sensitivity of estimating k_{iso} in this way to the combination of *both* δ_{sw} and the inlet conditions. Equivalent values of δ_{eq} calculated (Eq. 11) from $\delta_{sw,ce}$ between 0 and 5 cm were -6.15 ± 0.11, -3.57 ± 0.36 and 0.05 ± 0.07 ‰ $VPDB_g$ for the $\delta_{iw,low}$, $\delta_{iw,med}$, and $\delta_{iw,high}$ treatments, respectively. Means for k_{iso} estimated in this way using measurements made at $\delta_{b,low}$ were 0.042 ± 0.005, 0.029 ± 0.008 and 0.035 ± 0.003 s^{-1} for the $\delta_{iw,low}$, $\delta_{iw,med}$, and $\delta_{iw,high}$ treatments, respectively. These rates are roughly half the size of k_{iso} estimated from regression among multiple inlet conditions (Table 3). Positive
15 solutions for k_{iso} estimated using measurements made at $\delta_{b,med}$ were not found for all incubations and estimates were smaller still with means of 0.006 ± 0.002, 0.008 ± 0.005 and 0.015 ± 0.004 s^{-1} for the $\delta_{iw,low}$ ($n = 3$), $\delta_{iw,med}$ ($n = 5$) and $\delta_{iw,high}$ ($n = 6$) treatments, respectively. No solution was found for k_{iso} estimated using measurements made at $\delta_{b,high}$ for the $\delta_{iw,med}$ and $\delta_{iw,high}$ water treatments, whilst the estimates for $\delta_{iw,low}$ water treatment were two orders of magnitude larger with a mean of 3.18 ± 2.6 s^{-1}, i.e. more than 500 times larger than the un-catalysed rate. Situations where no solution are found arise in cases where
20 $(\delta_{eq} - \delta_R)(\delta_{eq} - \delta_a) \geq 0$. These cases and the considerable variability in k_{iso} among water treatments under different inlet conditions reflect the presence of an asymptote in the model response when δ_{eq} and δ_a are similar (Eq. 1). In this region of the response, relatively small changes in δ_{eq} result in large changes in k_{iso} as seen among estimates for the $\delta_{iw,low}$ water treatment made using $\delta_{b,low}$, $\delta_{b,med}$ and $\delta_{b,high}$ conditions (Fig. 6). From this analysis we can see that this can be problematic when attempts to estimate k_{iso} are made under field conditions. The oxygen isotopic composition of atmospheric CO_2 typically
25 ranges from -1.5 to +1.5 ‰ $VPDB_g$ (Welp et al., 2011). The isotopic composition of superficial soil water varies as a function of latitudinal and altitudinal patterns in the composition of precipitation and the subsequent influence of evapotranspiration, but is frequently reported in the range of -10 to +5 ‰VSMOW (Barbeta et al., 2015; Brooks et al., 2010; Dawson et al., 2002; Hsieh et al., 1998a). This suggests that values of δ_{eq}, after accounting for the influence of soil temperature and difference between scales in converting from δ_{sw} (Eq.11), can overlap the $\delta^{18}O$ of atmospheric CO_2 under
30 normal conditions (Wingate et al., 2009).

5 Conclusions

We have demonstrated that a strong linear correlation existed between δ_R and δ_a, suggesting that we should also be able to derive k_{iso} and $\delta_{sw,eq}$ from only two inlet conditions. This is beneficial, as it is likely to reduce the uncertainty in these estimates introduce by temporal changes in the CO_2 flux. We also reported an offset between $\delta_{sw,ce}$ and $\delta_{sw,eq}$ which indicates that bulk soil water may not always be the principal pool of interaction for CO_2. Such an offset might be explained by an isotopic fractionation between bound and bulk water pools, with the sign of this offset seeming to indicate that CO_2 interacts preferentially with bound water under our experiment conditions. Clearly, a better understanding of fine-scale heterogeneity in soil water isotope composition and microbial activity is required. Finally, our estimates of k_{iso} were independent of the isotopic composition of the irrigation water used, suggesting our approach is a robust assay of the activity, even in soils with low CA activities as reported here. Given the sensitivity of k_{iso} when estimated using a single CO_2 composition and prescribed vales of δ_{eq}, our approach clearly represents a more conservative and robust method. To better understand the cycling of oxygen isotopes of CO_2 within soils, further work is required to understand the physical processes controlling fractionation between soil water pools and the relation of CO_2 transport, microbial communities and their activity to these pools.

Author contributions

S.J, J.O, J.S, T. L, A. B. & L.W. developed the modelling and data processing approach.
S.W., J.S. and S.J. designed and built the gas exchange system.
S.J. and S.W. conducted gas flux measurements.
N.S , N.F, J.M, and S.J. tested the water extraction system and analysis system and conducted the soil water extractions and water analysis.
S.J. wrote the manuscript with contributions from all authors.

Acknowledgements

We would like to thank Régis Burlett, Callum Tyler, Thomas Sajus, and Jason West for their input in the laboratory and development of the experiment. This project has received funding from the European Research Council (ERC) under the European Union's Seventh Framework Programme (FP7/2007-2013) (grant agreement No. 338264) awarded to L.W. Salary for J.S. was funded by the Agence Nationale de la Recherche (ANR, project ORCA) and the INRA departments EA and EFPA.

References

Badger, M.: The roles of carbonic anhydrases in photosynthetic CO_2 concentrating mechanisms, Photosynthesis Research, 77(2-3), 83, doi:10.1023/A:1025821717773, 2003.

5 Badger, M. R. and Price, G. D.: The Role of Carbonic Anhydrase in Photosynthesis, Annual Review of Plant Physiology and Plant Molecular Biology, 45(1), 369–392, doi:10.1146/annurev.pp.45.060194.002101, 1994.

Banks, E. D., Taylor, N. M., Gulley, J., Lubbers, B. R., Giarrizzo, J. G., Bullen, H. A., Hoehler, T. M. and Barton, H. A.: Bacterial Calcium Carbonate Precipitation in Cave Environments: A Function of Calcium Homeostasis, Geomicrobiology
10 Journal, 27(5), 444–454, doi:10.1080/01490450903485136, 2010.

Barbeta, A., Mejía-Chang, M., Ogaya, R., Voltas, J., Dawson, T. E. and Peñuelas, J.: The combined effects of a long-term experimental drought and an extreme drought on the use of plant-water sources in a Mediterranean forest, Global Change Biology, 21(3), 1213–1225, doi:10.1111/gcb.12785, 2015.

Bates, D., Mächler, M., Bolker, B. and Walker, S.: Fitting Linear Mixed-Effects Models Using lme4, Journal of Statistical Software, 67(1), 1–48, doi:10.18637/jss.v067.i01, 2015.

Berman, E. S. F., Levin, N. E., Landais, A., Li, S. and Owano, T.: Measurement of $\delta18O$, $\delta17O$, and 17O-excess in Water by
20 Off-Axis Integrated Cavity Output Spectroscopy and Isotope Ratio Mass Spectrometry, Analytical Chemistry, 85(21), 10392–10398, doi:10.1021/ac402366t, 2013.

Birch, H. F.: The effect of soil drying on humus decomposition and nitrogen availability, Plant and Soil, 10(1), 9–31, doi:10.1007/BF01343734, 1958.

Bowling, D. R., Sargent, S. D., Tanner, B. D. and Ehleringer, J. R.: Tunable diode laser absorption spectroscopy for stable isotope studies of ecosystem–atmosphere CO_2 exchange, Agricultural and Forest Meteorology, 118(1–2), 1–19, doi:10.1016/S0168-1923(03)00074-1, 2003.

30 Brenninkmeijer, C. A. M., Kraft, P. and Mook, W. G.: Oxygen isotope fractionation between CO_2 and H_2O, Chemical Geology, 41, 181–190, doi:10.1016/S0009-2541(83)80015-1, 1983.

Brooks, J. R., Barnard, H. R., Coulombe, R. and McDonnell, J. J.: Ecohydrologic separation of water between trees and streams in a Mediterranean climate, Nature Geoscience, 3(2), 100–104, doi:10.1038/ngeo722, 2010.

5   Carrio, J. H.: Allanvar: Allan Variance Analysis, [online] Available from: https://CRAN.R-project.org/package=allanvar, 2015.

Chen, G., Auerswald, K. and Schnyder, H.: 2H and 18O depletion of water close to organic surfaces, Biogeosciences, 13(10), 3175–3186, doi:10.5194/bg-13-3175-2016, 2016.

Ciais, P., Sabine, C., Bala, G., Bopp, L., Brovkin, V., Canadell, J., Chhabra, A., DeFries, R., Galloway, J., Heimann, M., Jones, C., Le Quéré, C., Myneni, R., Piao, S. and Thornton, P.: Carbon and Other Biogeochemical Cycles, in Climate Change 2013: The Physical Science Basis. Contribution of Working Group I to the Fifth Assessment Report of the Intergovernmental Panel on Climate Change, edited by T. Stocker, D. Qin, G.-K. Plattner, M. Tignor, S. Allen, J. Boschung, A. Nauels, Y. Xia,
15   V. Bex, and P. Midgley, pp. 465–570, Cambridge University Press, Cambridge, United Kingdom; New York, NY, USA. [online] Available from: www.climatechange2013.org, 2013.

Crawley, M. J.: The R Book, Wiley, Chichester, West Sussex, United Kingdom, 2007.

20   Dawson, T. E., Mambelli, S., Plamboeck, A. H., Templer, P. H. and Tu, K. P.: Stable isotopes in plant ecology, Annual Review of Ecological Systems., 33(1), 507–559, doi:10.1146/annurev.ecolsys.33.020602.095451, 2002.

Farquhar, G. D., Lloyd, J., Taylor, J. A., Flanagan, L. B., Syvertsen, J. P., Hubick, K. T., Wong, S. C. and Ehleringer, J. R.: Vegetation effects on the isotope composition of oxygen in atmospheric CO_2, Nature, 363(6428), 439–443,
25   doi:10.1038/363439a0, 1993.

Francey, R. J. and Tans, P. P.: Latitudinal variation in oxygen-18 of atmospheric CO_2, Nature, 327(6122), 495–497, doi:10.1038/327495a0, 1987.

30   Geldern, R. van, Nowak, M. E., Zimmer, M., Szizybalski, A., Myrttinen, A., Barth, J. A. C. and Jost, H.-J.: Field-Based Stable Isotope Analysis of Carbon Dioxide by Mid-Infrared Laser Spectroscopy for Carbon Capture and Storage Monitoring, Analytical Chemistry, 86(24), 12191–12198, doi:10.1021/ac5031732, 2014.

Gillon, J. and Yakir, D.: Influence of Carbonic Anhydrase Activity in Terrestrial Vegetation on the 18O Content of Atmospheric CO2, Science, 291(5513), 2584–2587, doi:10.1126/science.1056374, 2001.

5 Gilmour, K. M.: Perspectives on carbonic anhydrase, Comparative Biochemistry and Physiology Part A: Molecular & Integrative Physiology, 157(3), 193–197, doi:10.1016/j.cbpa.2010.06.161, 2010.

Hewett-Emmett, D. and Tashian, R. E.: Functional Diversity, Conservation, and Convergence in the Evolution of the α-, β-, and γ-Carbonic Anhydrase Gene Families, Molecular Phylogenetics and Evolution, 5(1), 50–77,
10 doi:10.1006/mpev.1996.0006, 1996.

Hopkinson, B. M., Meile, C. and Shen, C.: Quantification of Extracellular Carbonic Anhydrase Activity in Two Marine Diatoms and Investigation of Its Role, Plant Physiology, 162(2), 1142–1152, doi:10.1104/pp.113.217737, 2013.

15 Hsieh, J. C., Chadwick, O. A., Kelly, E. F. and Savin, S. M.: Oxygen isotopic composition of soil water: Quantifying evaporation and transpiration, Geoderma, 82(1-3), 269–293, doi:10.1016/S0016-7061(97)00105-5, 1998a.

Hsieh, J. C. C., Savin, S. M., Kelly, E. F. and Chadwick, O. A.: Measurement of soil-water δ18O values by direct equilibration with CO2, Geoderma, 82(1–3), 255–268, doi:10.1016/S0016-7061(97)00104-3, 1998b.

Jarvis, P., Rey, A., Petsikos, C., Wingate, L., Rayment, M., Pereira, J., Banza, J., David, J., Miglietta, F., Borghetti, M., Manca, G. and Valentini, R.: Drying and wetting of Mediterranean soils stimulates decomposition and carbon dioxide emission: The "Birch effect", Tree Physiology, 27(7), 929–940, doi:10.1093/treephys/27.7.929, 2007.

25 Kapiluto, Y., Yakir, D., Tans, P. and Berkowitz, B.: Experimental and numerical studies of the 18O exchange between CO2 and water in the atmosphere–soil invasion flux, Geochimica et Cosmochimica Acta, 71(11), 2657–2671, doi:10.1016/j.gca.2007.03.016, 2007.

Kaur, S., Mishra, M. N. and Tripathi, A. K.: Regulation of expression and biochemical characterization of a β-class carbonic
30 anhydrase from the plant growth-promoting rhizobacterium, Azospirillum brasilense Sp7, FEMS Microbiology Letters, 299(2), 149–158, doi:10.1111/j.1574-6968.2009.01736.x, 2009.

Lebeau, M. and Konrad, J.-M.: A new capillary and thin film flow model for predicting the hydraulic conductivity of unsaturated porous media, Water Resources Research, 46(12), W12554, doi:10.1029/2010WR009092, 2010.

Li, W., Yu, L.-j., Yuan, D.-x., Wu, Y. and Zeng, X.-d.: A study of the activity and ecological significance of carbonic anhydrase from soil and its microbes from different karst ecosystems of Southwest China, Plant and Soil, 272(1-2), 133–141, doi:10.1007/s11104-004-4335-9, 2005a.

Li, W., Yu, L.-j., He, Q.-f., Wu, Y., Yuan, D.-x. and Cao, J.-h.: Effects of microbes and their carbonic anhydrase on Ca2+ and Mg2+ migration in column-built leached soil-limestone karst systems, Applied Soil Ecology, 29(3), 274–281, doi:10.1016/j.apsoil.2004.12.001, 2005b.

Lin, Y. and Horita, J.: An experimental study on isotope fractionation in a mesoporous silica-water system with implications for vadose-zone hydrology, Geochimica et Cosmochimica Acta, 184, 257–271, doi:10.1016/j.gca.2016.04.029, 2016.

Linn, D. M. and Doran, J. W.: Effect of Water-Filled Pore Space on Carbon Dioxide and Nitrous Oxide Production in Tilled and Nontilled Soils, Soil Science Society of America Journal, 48(6), 1267–1272, doi:10.2136/sssaj1984.03615995004800060013x, 1984.

Lis, G., Wassenaar, L. I. and Hendry, M. J.: High-Precision Laser Spectroscopy D/H and 18O/16O Measurements of Microliter Natural Water Samples, Analytical Chemistry, 80(1), 287–293, doi:10.1021/ac701716q, 2008.

Massman, W. J.: A review of the molecular diffusivities of H2O, CO2, CH4, CO, O3, SO2, NH3, N2O, NO, and NO2 in air, O2 and N2 near STP, Atmospheric Environment, 32(6), 1111–1127, doi:10.1016/S1352-2310(97)00391-9, 1998.

Mendiburu, F. de: Agricolae: Statistical Procedures for Agricultural Research. [online] Available from: https://CRAN.R-project.org/package=agricolae, 2016.

Merlin, C., Masters, M., McAteer, S. and Coulson, A.: Why Is Carbonic Anhydrase Essential to Escherichia coli?, Journal of Bacteriology, 185(21), 6415–6424, doi:10.1128/JB.185.21.6415-6424.2003, 2003.

Miller, J. B., Yakir, D., White, J. W. C. and Tans, P. P.: Measurement of 18O/16O in the soil-atmosphere CO2 flux, Global Biogeochemical Cycles, 13(3), 761–774, doi:10.1029/1999GB900028, 1999.

Mills, G. A. and Urey, H. C.: The Kinetics of Isotopic Exchange between Carbon Dioxide, Bicarbonate Ion, Carbonate Ion and Water1, Journal of the American Chemical Society, 62(5), 1019–1026, doi:10.1021/ja01862a010, 1940.

5 Moldrup, P., Olesen, T., Komatsu, T., Yoshikawa, S., Schjønning, P. and Rolston, D.: Modeling diffusion and reaction in soils: X. A unifying model for solute and gas diffusivity in unsaturated soil, Soil Science, 168(5), 321–337, 2003.

Oerter, E., Finstad, K., Schaefer, J., Goldsmith, G. R., Dawson, T. and Amundson, R.: Oxygen isotope fractionation effects in soil water via interaction with cations (Mg, Ca, K, Na) adsorbed to phyllosilicate clay minerals, Journal of Hydrology, 515, 10 1–9, doi:10.1016/j.jhydrol.2014.04.029, 2014.

Ogée, J., Peylin, P., Cuntz, M., Bariac, T., Brunet, Y., Berbigier, P., Richard, P. and Ciais, P.: Partitioning net ecosystem carbon exchange into net assimilation and respiration with canopy-scale isotopic measurements: An error propagation analysis with 13CO2 and CO18O data, Global Biogeochemical Cycles, 18(2), GB2019, doi:10.1029/2003GB002166, 2004.

Ogée, J., Sauze, J., Kesselmeier, J., Genty, B., Van Diest, H., Launois, T. and Wingate, L.: A new mechanistic framework to predict OCS fluxes from soils, Biogeosciences, 13(8), 2221–2240, doi:10.5194/bg-13-2221-2016, 2016.

Orlowski, N., Frede, H.-G., Brüggemann, N. and Breuer, L.: Validation and application of a cryogenic vacuum extraction 20 system for soil and plant water extraction for isotope analysis, Journal of Sensors and Sensor Systems, 2(2), 179–193, doi:10.5194/jsss-2-179-2013, 2013.

Orlowski, N., Breuer, L. and McDonnell, J. J.: Critical issues with cryogenic extraction of soil water for stable isotope analysis, Ecohydrology, 9(1), 1–5, doi:10.1002/eco.1722, 2016a.

Orlowski, N., Pratt, D. L. and McDonnell, J. J.: Intercomparison of soil pore water extraction methods for stable isotope analysis, Hydrological Processes, 30(19), 3434–3449, doi:10.1002/hyp.10870, 2016b.

R Core Team: R: A Language and Environment for Statistical Computing, R Foundation for Statistical Computing, Vienna, 30 Austria. [online] Available from: https://www.R-project.org/, 2017.

Riley, W. J.: A modeling study of the impact of the δ18O value of near-surface soil water on the δ18O value of the soil-surface CO2 flux, Geochimica et Cosmochimica Acta, 69(8), 1939–1946, doi:10.1016/j.gca.2004.10.021, 2005.

Rizzo, A. L., Jost, H.-J., Caracausi, A., Paonita, A., Liotta, M. and Martelli, M.: Real-time measurements of the concentration and isotope composition of atmospheric and volcanic CO2 at Mount Etna (Italy), Geophysical Research Letters, 41(7), 2014GL059722, doi:10.1002/2014GL059722, 2014.

Savin, S. M. and Epstein, S.: The oxygen and hydrogen isotope geochemistry of clay minerals, Geochimica et Cosmochimica Acta, 34(1), 25–42, doi:10.1016/0016-7037(70)90149-3, 1970.

Seibt, U., Wingate, L., Lloyd, J. and Berry, J. A.: Diurnally variable δ18O signatures of soil CO2 fluxes indicate carbonic anhydrase activity in a forest soil, Journal of Geophysical Research: Biogeosciences, 111(G4), G04005, doi:10.1029/2006JG000177, 2006.

Smith, K. S. and Ferry, J. G.: Prokaryotic carbonic anhydrases, FEMS Microbiology Reviews, 24(4), 335–366, doi:10.1111/j.1574-6976.2000.tb00546.x, 2000.

Smith, K. S., Jakubzick, C., Whittam, T. S. and Ferry, J. G.: Carbonic anhydrase is an ancient enzyme widespread in prokaryotes, Proceedings of the National Academy of Sciences, 96(26), 15184–15189, doi:10.1073/pnas.96.26.15184, 1999.

Sprenger, M., Herbstritt, B. and Weiler, M.: Established methods and new opportunities for pore water stable isotope analysis, Hydrological Processes, 29(25), 5174–5192, doi:10.1002/hyp.10643, 2015.

Stern, L. A., Amundson, R. and Baisden, W. T.: Influence of soils on oxygen isotope ratio of atmospheric CO2, Global Biogeochemical Cycles, 15(3), 753–759, doi:10.1029/2000GB001373, 2001.

Tans, P. P.: Oxygen isotopic equilibrium between carbon dioxide and water in soils, Tellus B, 50(2), doi:10.3402/tellusb.v50i2.16094, 1998.

Tokunaga, T. K.: Physicochemical controls on adsorbed water film thickness in unsaturated geological media, Water Resources Research, 47(8), W08514, doi:10.1029/2011WR010676, 2011.

Tu, C., Wynns, G. C., McMurray, R. E. and Silverman, D. N.: CO2 kinetics in red cell suspensions measured by 18O exchange., Journal of Biological Chemistry, 253(22), 8178–8184 [online] Available from: http://www.jbc.org/content/253/22/8178 (Accessed 28 September 2016), 1978.

5 Tuller, M. and Or, D.: Hydraulic conductivity of variably saturated porous media: Film and corner flow in angular pore space, Water Resources Research, 37(5), 1257–1276, doi:10.1029/2000WR900328, 2001.

Uchikawa, J. and Zeebe, R. E.: The effect of carbonic anhydrase on the kinetics and equilibrium of the oxygen isotope exchange in the CO2–H2O system: Implications for δ18O vital effects in biogenic carbonates, Geochimica et Cosmochimica
10 Acta, 95, 15–34, doi:10.1016/j.gca.2012.07.022, 2012.

Weiss, R. F.: Carbon dioxide in water and seawater: The solubility of a non-ideal gas, Marine Chemistry, 2(3), 203–215, doi:10.1016/0304-4203(74)90015-2, 1974.

15 Welp, L. R., Keeling, R. F., Meijer, H. A. J., Bollenbacher, A. F., Piper, S. C., Yoshimura, K., Francey, R. J., Allison, C. E. and Wahlen, M.: Interannual variability in the oxygen isotopes of atmospheric CO2 driven by El Nino, Nature, 477(7366), 579–582, doi:10.1038/nature10421, 2011.

Wen, X.-F., Meng, Y., Zhang, X.-Y., Sun, X.-M. and Lee, X.: Evaluating calibration strategies for isotope ratio infrared
20 spectroscopy for atmospheric 13CO2 / 12CO2 measurement, Atmos. Meas. Tech., 6(6), 1491–1501, doi:10.5194/amt-6-1491-2013, 2013.

Werle, P.: Accuracy and precision of laser spectrometers for trace gas sensing in the presence of optical fringes and atmospheric turbulence, Applied Physics B, 102(2), 313–329, doi:10.1007/s00340-010-4165-9, 2010.
25
Wilbur, K. M. and Anderson, N. G.: Electrometric and Colorimetric Determination of Carbonic Anhydrase, Journal of Biological Chemistry, 176(1), 147–154 [online] Available from: http://www.jbc.org/content/176/1/147 (Accessed 28 September 2016), 1948.

30 Wingate, L., Seibt, U., Maseyk, K., Ogée, J., Almeida, P., Yakir, D., Pereira, J. S. and Mencuccini, M.: Evaporation and carbonic anhydrase activity recorded in oxygen isotope signatures of net CO2 fluxes from a Mediterranean soil, Global Change Biology, 14(9), 2178–2193, doi:10.1111/j.1365-2486.2008.01635.x, 2008.

Wingate, L., Ogée, J., Cuntz, M., Genty, B., Reiter, I., Seibt, U., Yakir, D., Maseyk, K., Pendall, E. G., Barbour, M. M., Mortazavi, B., Burlett, R., Peylin, P., Miller, J., Mencuccini, M., Shim, J. H., Hunt, J. and Grace, J.: The impact of soil microorganisms on the global budget of δ18O in atmospheric CO2, Proceedings of the National Academy of Sciences, 5 106(52), 22411–22415, doi:10.1073/pnas.0905210106, 2009.

Wingate, L., Ogée, J., Burlett, R. and Bosc, A.: Strong seasonal disequilibrium measured between the oxygen isotope signals of leaf and soil CO2 exchange, Global Change Biology, 16(11), 3048–3064, doi:10.1111/j.1365-2486.2010.02186.x, 2010.

10 Xu, Y., Feng, L., Jeffrey, P. D., Shi, Y. and Morel, F. M. M.: Structure and metal exchange in the cadmium carbonic anhydrase of marine diatoms, Nature, 452(7183), 56–61, doi:10.1038/nature06636, 2008.

Yakir, D. and Wang, X.-F.: Fluxes of CO2 and water between terrestrial vegetation and the atmosphere estimated from isotope measurements, Nature, 380(6574), 515–517, doi:10.1038/380515a0, 1996.

Tables

Table 1: Soil properties by irrigation water treatment (δ_{iw}). Means (n = 6) and standard deviations (in parentheses) for bulk density, soil depth (z_{max}), total porosity (ϕ_t), volumetric soil water content (θ_w), and tortuoisity (κ). Lower-case letters indicate significant differences (one-way analysis of variance and Tukey's HSD, $p < 0.01$) among δ_{iw} treatments.

Treatment	Bulk density (g cm^{-3})	z_{max} (mm)	ϕ_t	θ_w	κ
$\delta_{iw,low}$	1.06 (0.03) a	60.3 (1.5) a	0.599 (0.010) a	0.112 (0.002) a	0.57 (0.1) a
$\delta_{iw,med}$	1.04 (0.01) a	61.5 (0.8) a	0.607 (0.004) a	0.110 (0.002) a	0.58 (0.01) a
$\delta_{iw,high}$	1.06 (0.03) a	60.3 (1.4) a	0.599 (0.009) a	0.112 (0.002) a	0.57 (0.01) a

Table 2: Gas exchange data by irrigation water (δ_{iw}) treatment at the three different incubation system inlet conditions (δ_b). Means and standard deviations (in parenthesis) for total CO_2 concentration in the bypass (C_b) and the chamber (C_a), the $\delta^{18}O$ of CO_2 in the bypass (δ_b) and the chamber (δ_a), and the net flux of CO_2 (F_R) and its $\delta^{18}O$ (δ_R).

	$\delta_{iw,low}$			$\delta_{iw,med}$			$\delta_{iw,high}$		
	$\delta_{b,low}$	$\delta_{b,med}$	$\delta_{b,high}$	$\delta_{b,low}$	$\delta_{b,med}$	$\delta_{b,high}$	$\delta_{b,low}$	$\delta_{b,med}$	$\delta_{b,high}$
C_b	425.99	423.80	425.06	424.24	422.82	425.04	425.73	422.23	425.08
(ppm)	(1.35)	(0.92)	(0.04)	(1.74)	(0.99)	(0.14)	(1.50)	(0.83)	(0.03)
C_a	482.13	480.28	481.24	495.26	494.20	496.78	488.80	485.06	488.01
(ppm)	(9.79)	(8.56)	(6.39)	(11.09)	(12.71)	(14.59)	(3.93)	(3.52)	(2.87)
F_R	1.98	1.99	1.98	2.50	2.51	2.53	2.22	2.21	2.22
(μmol m^{-2} s^{-1})	(0.31)	(0.30)	(0.23)	(0.43)	(0.42)	(0.52)	(0.17)	(0.12)	(0.10)
δ_b	−26.80	−13.92	−3.63	−26.87	−13.97	−3.62	−26.86	−13.99	−3.58
(‰ VPDB$_g$)	(0.25)	(0.09)	(0.15)	(0.22)	(0.17)	(0.30)	(0.06)	(0.08)	(0.11)
δ_a	−22.48	−13.01	−5.56	−21.90	−12.36	−5.11	−21.12	−11.62	−4.20
(‰ VPDB$_g$)	(0.26)	(0.10)	(0.19)	(0.34)	(0.09)	(0.51)	(0.23)	(0.10)	(0.17)
δ_R	10.80	−6.05	−20.27	8.34	−2.67	−14.01	17.73	4.40	−8.36
(‰ VPDB$_g$)	(3.70)	(1.22)	(0.95)	(3.83)	(1.12)	(1.33)	(2.03)	(1.18)	(0.74)

Table 3: Model solutions by irrigation water (δ_{iw}) treatment. Means (n = 6) and standard deviations (in parenthesis) for the piston velocity of CO_2 assuming a semi-infinite soil depth (v_{inv}), the piston velocity of CO_2 assuming a finite soil depth ($\tilde{v}_{inv}$), the apparent rate of exchange between CO_2 and soil water (k_{iso}), the effective diffusional fraction of CO_2 assuming a finite soil depth ($\tilde{a}$), and the $\delta^{18}O$ of soil water in equilibrium with CO_2 as determined from gas flux measurements ($\delta_{sw,eq}$). Lower-case letters indicate significant differences (one-way analysis of variance and Tukey's HSD, $p < 0.01$) among δ_{iw} treatments.

Treatment	v_{inv} (mm s^{-1})	$\tilde{v}_{inv}$ (mm s^{-1})	k_{iso} (s^{-1})	$\tilde{a}$ (‰ VPDB$_g$)	$\delta_{sw,eq}$ (‰ VSMOW-SLAP)
$\delta_{iw,low}$	0.179 (0.011) a	0.181 (0.011) a	0.080 (0.009) a	5.36 (0.16) a	-9.31 (0.20) c
$\delta_{iw,med}$	0.158 (0.021) a	0.162 (0.02) a	0.063 (0.015) a	4.88 (0.43) a	-7.04 (0.52) b
$\delta_{iw,high}$	0.168 (0.014) a	0.171 (0.013) a	0.071 (0.012) a	5.14 (0.29) a	-4.16 (0.18) a

Figures
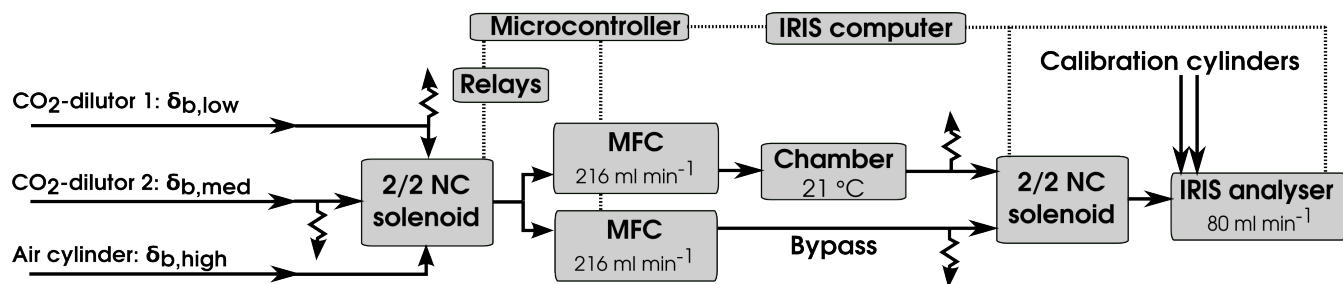
Figure 1: Schematic of the system used to make gas exchange measurements. Alternate measurements of the concentration and $\delta^{18}O$ of CO_2 in chamber (C_a, δ_a) and bypass lines (C_b, δ_b) are made under three inlet conditions ($\delta_{b,low}$, $\delta_{b,med}$, $\delta_{b,high}$) that differ in terms of the $\delta^{18}O$ of CO_2.
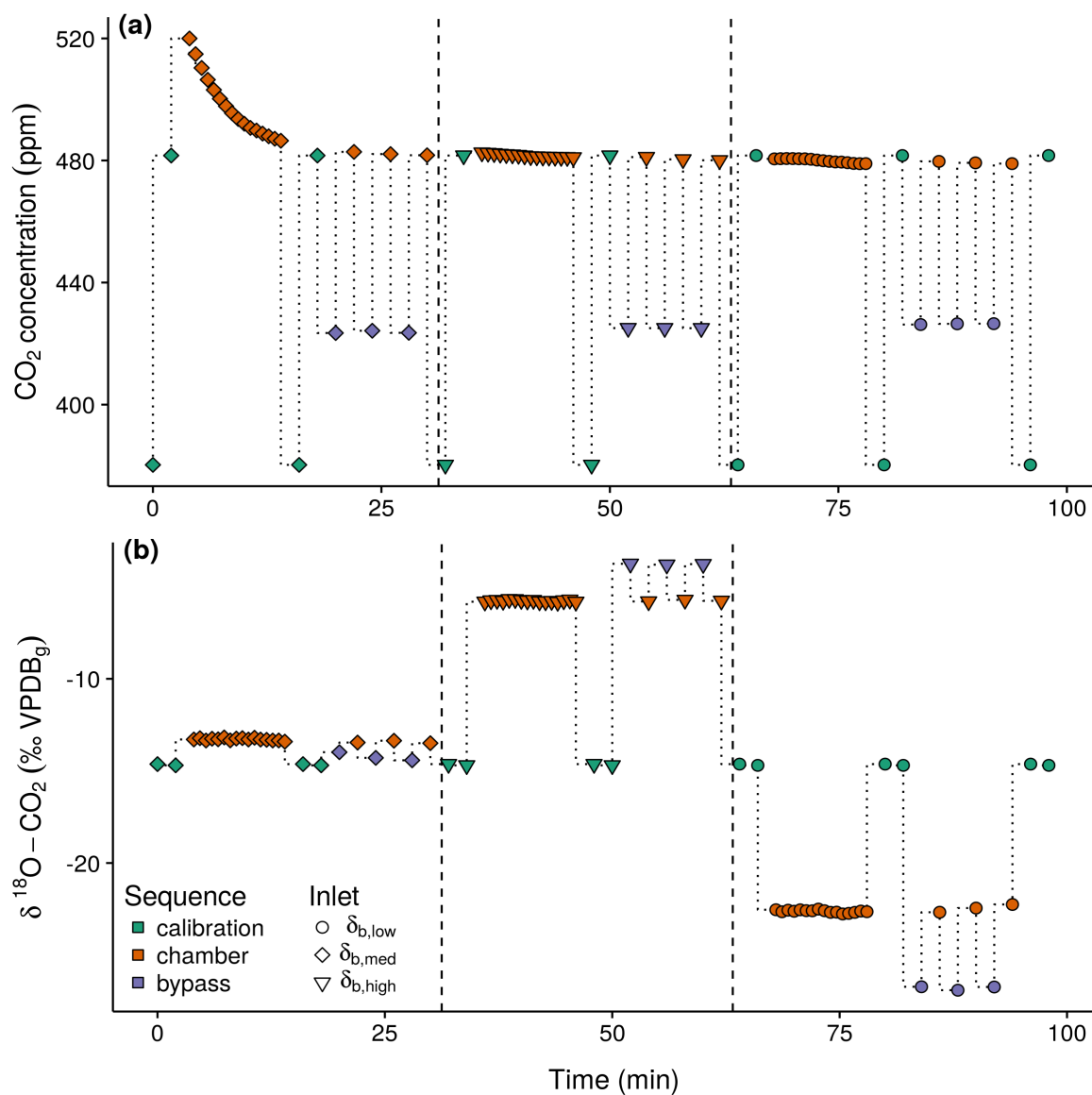
Figure 2: An example of the gas exchange measurement sequence, scanning sequentially calibration cylinders, the chamber line during a stabilisation period, calibration cylinders again, and finally the chamber and bypass lines, for the three different $\delta^{18}O$ of CO_2 delivered to the inlet of the incubation system (δ_b). In this case, the δ_b inlet conditions, whose changes are indicated by the vertical dashed lines, started with $\delta_{b,med}$ and ended with $\delta_{b,low}$. Symbols represent the calibrated average values and the dotted line is provided as a visual aid and does not correspond to raw 1-Hz data, (a) total CO_2 concentration and, (b) $\delta^{18}O$ of CO_2.
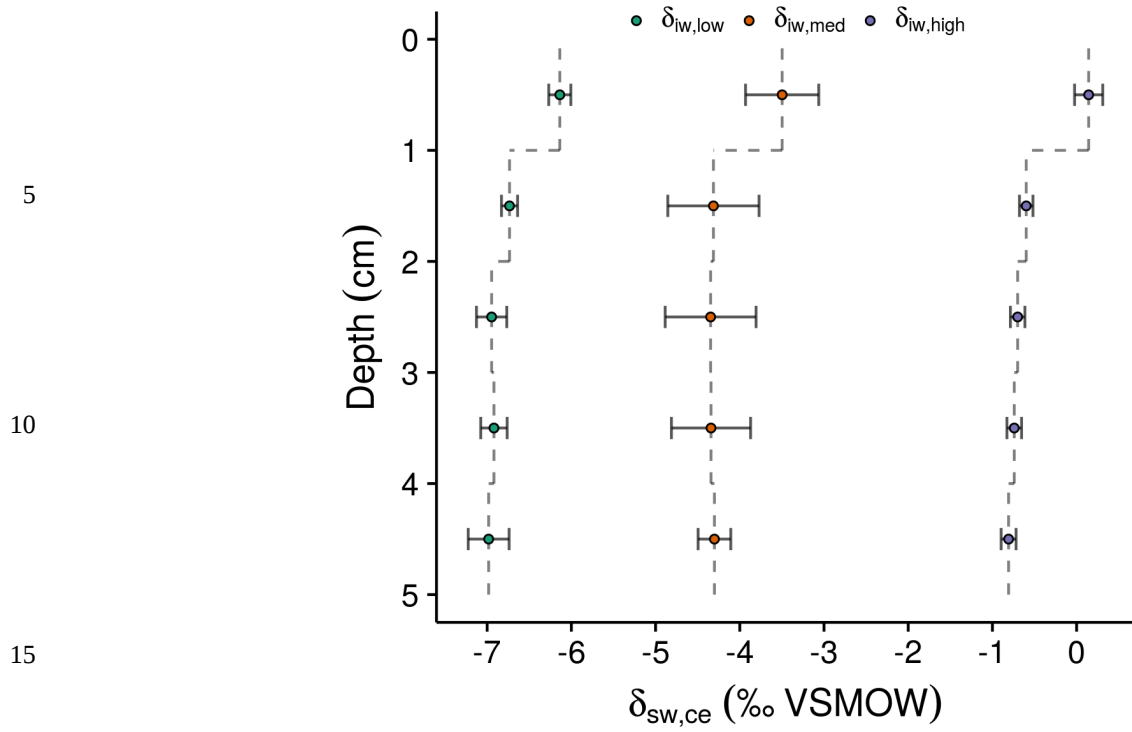
Figure 3: Incubation depth profiles of the $\delta^{18}O$ of cryogenically extracted soil water ($\delta_{sw,ce}$), at intervals of 0-1, 1-2, 2-3, and 4-5 cm below the surface. Symbols and error bars indicate means and standard deviations by irrigation water (δ_{iw}) treatment and depth interval.
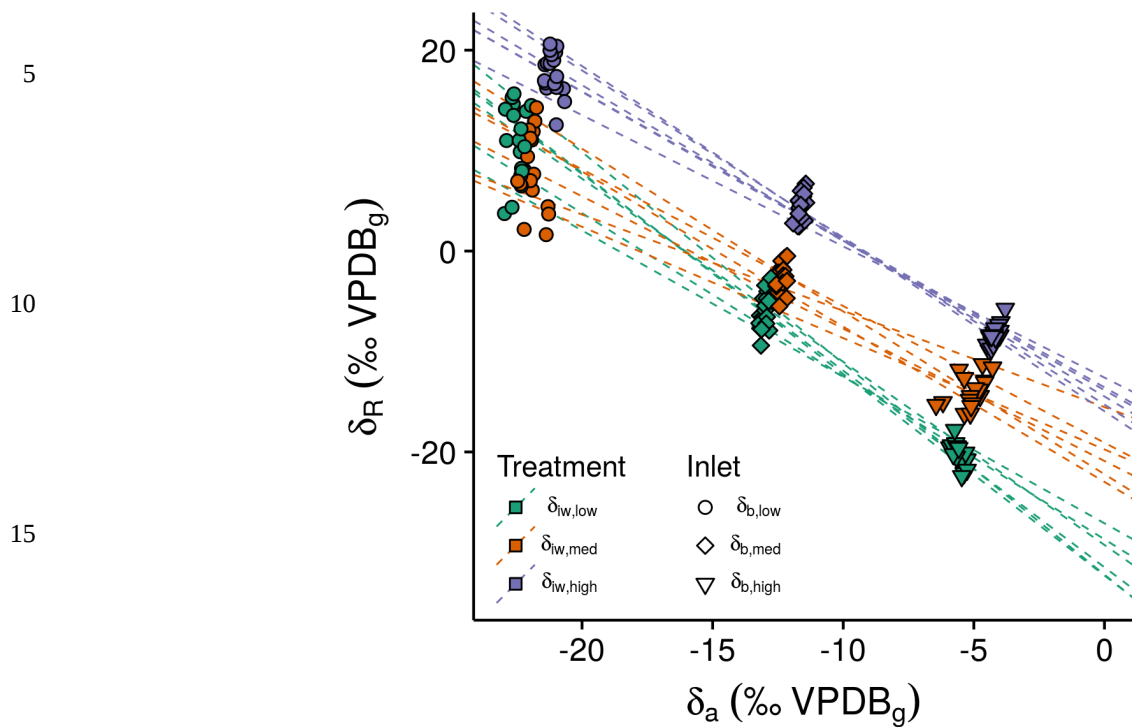
Figure 4: Relationships between the $\delta^{18}O$ of soil-atmosphere CO_2 exchange (δ_R) and the $\delta^{18}O$ of CO_2 in the chamber line (δ_a) by irrigation water (δ_{iw}) treatment. Symbol shapes indicate measurements made at different inlet conditions (δ_b) that varied in terms of their $\delta^{18}O$ of CO_2. Dashed lines indicate linear regressions for individual incubations.
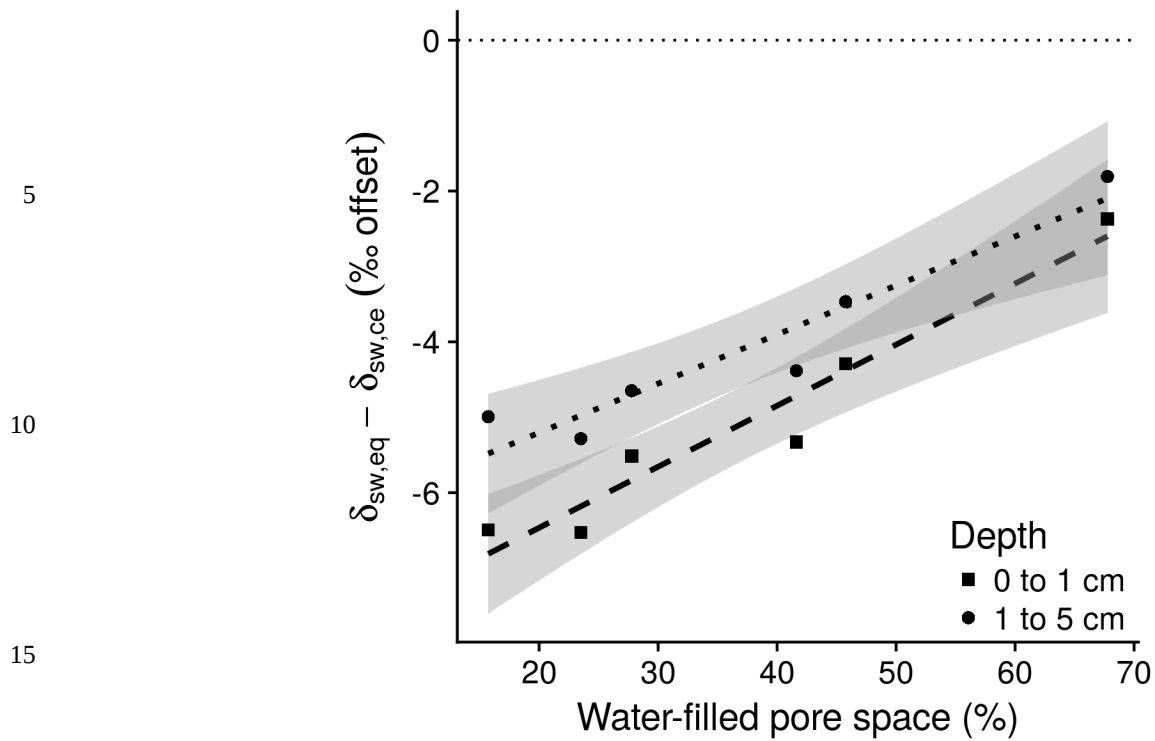
Figure 5: Relationships between water-filled pore space and the difference between estimates of the $\delta^{18}O$ of soil water in equilibrium with CO_2 as estimated from gas flux measurements ($\delta_{sw,eq}$) and that estimated by cryogenic extraction ($\delta_{sw,ce}$) at depths of 0-1 cm (squares) and 1-5 cm (circles). Dashed lines and shaded areas indicate the linear regressions and associated 95 % confidence intervals for the two sampling depths.
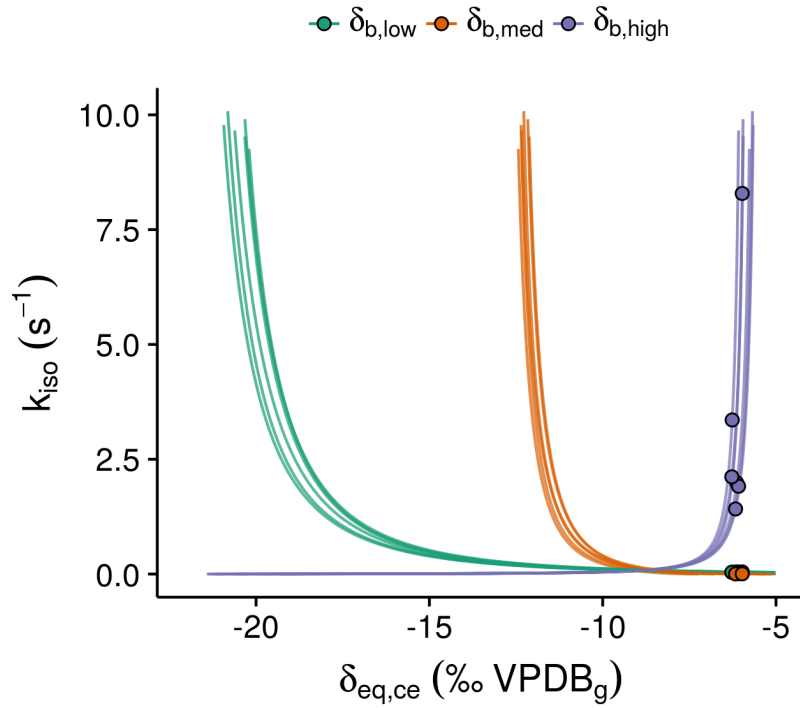
Figure 6: Model relationships between the apparent rate of exchange (k_{iso}) and the $\delta^{18}O$ of CO_2 in equilibrium with soil water ($\delta_{eq,ce}$). These $\delta_{eq,ce}$ values were assumed from the depth averaged $\delta^{18}O$ of cryogenically extracted water for the incubations that received the $\delta_{iw,low}$ ($\delta^{18}O$ of -6.74 ± 0.03 ‰ VSMOW-SLAP) irrigation water. Colours indicate the different responses for the same set of incubations at the three inlet conditions that differed by their $\delta^{18}O$ of CO_2 (δ_b).